non density we only need to use this feature to determine the occupation number $\bar{n}(E)$ by taking the ratio of the *modulated* anti-Stokes signal [Fig. 1(b)] to the *unmodulated* Stokes signal [Fig. 1(a)]. In taking this ratio, we have obtained the unmodulated Stokes signal at small E by assuming that the central peak is symmetric. The modulated anti-Stokes signal is corrected by assuming that the line shapes of the central peaks are the same in the modulated and the unmodulated spectra. The dashed curves in Fig. 1 are drawn according to this procedure.

A plot of this ratio $\Delta I(+E)/I(-E) = \bar{n}(E)$ versus E is shown in Fig. 2 for three different excitation levels.[10] The figure also shows solid curves calculated from $\bar{n}(E) = 1/[\exp(E/kT) - 1]$ for three different temperatures. We see that the agreement between the calculated curves and the experimental points is excellent, and conclude that the phonon distribution generated by photoexcitation of the gold film can be well described by a temperature. The temperature determined in this way is proportional to the fourth root of the incident power as expected for the temperature variation of the Au film. These observations demonstrate that the I_1 luminescence feature can be used as a phonon spectrometer.

The I_1 phonon spectrometer is ideally suited for measuring nonequilibrium phonon distributions. Examples include the phonon fluorescence spectra of superconductors and their variation with external perturbations such as magnetic fields. It should also be possible to study quantitatively the transmission of phonons at interfaces and the effect of selective absorption or scattering of phonons by impurities in CdS. The I_1 phonon spectrometer thus opens up a wide range of possibilities, some of which we are currently exploring.

We thank J. J. Hopfield and J. M. Worlock for useful discussions and E. Beebe, A. E. DiGiovanni, and J. J. Wiegand for technical assistance.

[1]D. G. Thomas and J. J. Hopfield, Phys. Rev. 128, 2135 (1962).

[2]R. C. Dynes and V. Narayanamurti, Phys. Rev. B 6, 143 (1972).

[3]C. H. Anderson, in *Physical Acoustics*, edited by W. P. Mason and R. N. Thurston (Academic, New York, 1972), Vol. 8, Chap. 1.

[4]C. H. Henry, K. Nassau, and J. W. Shiever, Phys. Rev. Lett. 24, 820 (1970).

[5]J. J. Hopfield, in *Proceedings of the International Conference on the Physics of Semiconductors, Exeter, 1962*, edited by A. C. Stickland (Bartholomew Press, Dorking, England, 1962), p. 75.

[6]C. H. Henry and K. Nassau, J. Lumines. 1,2, 299 (1970).

[7]Strong, sharp, I_1 emission lines can also be observed on cleaved faces of many bulk crystals or bulk crystals which are doped with Na or Li [B. Tell, J. Appl. Phys. 42, 2919 (1971)].

[8]4765-Å radiation is strongly absorbed by CdS whereas 5145 Å is not absorbed and does not affect the I_1 luminescence in any way.

[9]J. Shah, R. F. Leheny, and W. F. Brinkman, Phys. Rev. B 10, 659 (1974).

[10]The presence of I_2 luminescence $E = +11$ meV limits the range of measurement to about 4 meV. Removal of the impurities responsible for this feature would extend the range of the I_1 spectrometer to ≈ 12 meV, the cutoff energy for acoustic phonons in CdS.

Temperature- and Composition-Dependent Valence Mixing of Sm in Cation- and Anion-Substituted SmS Observed by X-ray Photoemission Spectroscopy*

R. A. Pollak, F. Holtzberg, J. L. Freeouf, and D. E. Eastman
IBM Thomas J. Watson Research Center, Yorktown Heights, New York 10598
(Received 17 June 1974)

We have determined the interconfiguration mixing ratios (Sm^{+3}/Sm^{+2}) of 1.4 and 4.1 for $Sm_{0.81}Y_{0.19}S$ and $SmAs_{0.18}S_{0.82}$ at 295 K from their x-ray photoemission spectra. These ratios are observed to decrease reversibly by a factor of 2 at 110 K. The agreement of these results with valences deduced from lattice-constant measurements is direct evidence that configuration mixing is responsible for the anomalous temperature- and composition-dependence of the lattice constant.

A mixture of two configurations within the ground-state eigenstate of SmS and its solid solutions has recently been correlated with many unique and unusual properties, including (1) the dramatic pressure-induced semiconducting-to-metal phase transformation in SmS[1] which is a

reversible isostructural transition from a black semiconducting phase with effective Sm valence of ~2 to a collapsed gold-colored phase with effective Sm valence of 2.77 ± 0.06 derived from the lattice constant,[2] (2) the concentration-dependent lattice collapse from a black to gold phase in cation-substituted ($Sm_{1-x}Gd_xS$,[3] $Sm_{1-x}Y_xS$,[3,4] and $Sm_{1-x}La_xS$[4]) and anion-substituted ($SmAs_xS_{1-x}$) SmS, and (3) the fact that in certain critical regions of solid solution, the collapsed gold-colored phase transforms upon cooling back to a black phase either as an explosive first-order transition or a continuous transition over a range of temperatures.[3,4] The configuration mixing in these systems is ascribed to conditions which produce the near degeneracy of the $Sm(4f^6) \equiv Sm^{+2}$ and the $Sm(4f^5 d_{\text{conduct}}^1) \equiv Sm^{+3}$ states.[5] The interconfiguration energy is the energy necessary to excite an electron from a localized $4f$ orbital of the former state to an intinerant d conduction band of the latter state. Because of the highly correlated nature of the localized $4f$ electrons, the extra energy necessary to remove another Sm $4f$ electron ($4f^5 \rightarrow 4f^4 + e^-$) is much larger (~6 eV) than the interconfiguration energy. It is this energy, the intraconfiguration or Coulomb correlation energy U, which separates the Sm $4f$ photoemission structures obtained from the nearly degenerate initial states of Sm^{+2} and Sm^{+3} and thus makes x-ray photoemission spectroscopy (XPS) with a resolution of 0.6 eV a suitable technique for directly obtaining interconfiguration mixing ratios from the electronic density of states.

Previously, the Mössbauer isomer shift and the soft x-ray absorption of SmB_6, and lattice-constant measurements of α-Ce, SmS ($P = 8$ kbar), and SmB_6[2] and ternary SmS solid solutions[4] have yielded a measure of the intermediate valence in these systems. Interconfiguration mixing has been observed in the XPS spectra of TmSe and TmTe where the Coulomb correlation energy was observed to be between 6.5 and 7 eV.[6]

We report the x-ray photoemission spectra of the outermost orbitals of YS, SmS, SmAs, $SmAs_{0.18}S_{0.82}$, and $Sm_{0.81}Y_{0.19}S$ shown in Fig. 1, assign their spectral features, and use observed $4f$ features to determine the effective intermediate valence and temperature-dependent change in valence for $SmAs_{0.18}S_{0.82}$ and $Sm_{0.81}Y_{0.19}S$. The XPS data were obtained with a Hewlett Packard 5950A photoelectron spectrometer which employs a monochromatic $K\alpha_{1,2}$ x-ray source. Single crystals ($6 \times 4 \times 2$ mm^3) whose preparation is described elsewhere[4] were cleaved in the 5×10^{-9}-Torr vacuum of the spectrometer's sample preparation chamber and then moved directly into the analyzer vacuum of less than 10^{-9} Torr. Even with a baked system at these high vacuums, the cleaved surfaces were moderately reactive and were oxidized with time, resulting in a steady conversion of divalent to trivalent samarium. To monitor and minimize the effects of such surface deterioration, Sm $3d$ spectra were taken immedi-

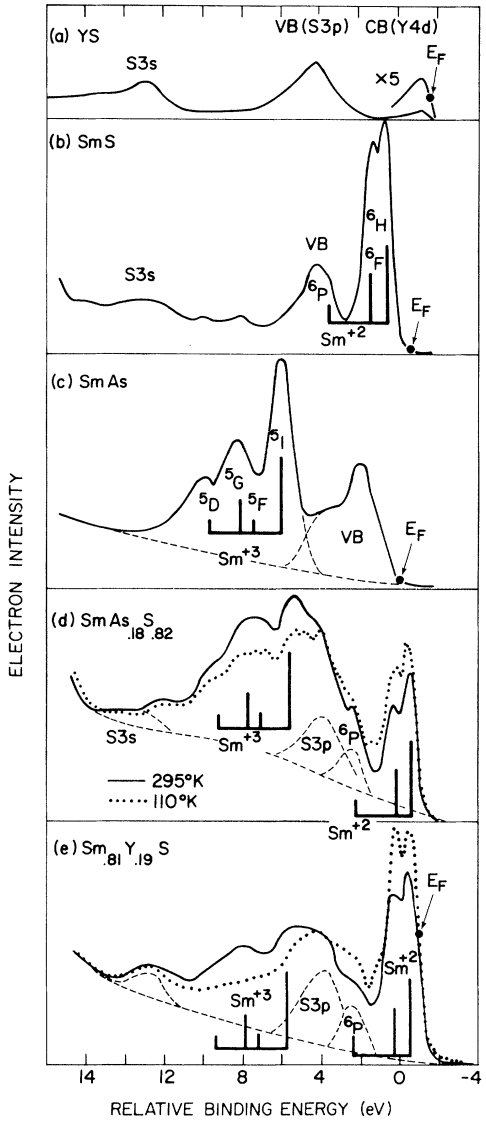

FIG. 1. X-ray photoemission spectra of (a) YS; (b) SmS; (c) SmAs; (d) $AmAs_{0.18}S_{0.82}$—295 K, solid line; 110 K, dotted line; and (e) $Sm_{0.81}Y_{0.19}S$—295 K, solid line; 110 K, dotted line. Dashed curves in (d) and (e) are components of the deconvoluted 295-K spectra.

ately after cleaving, valence spectra were recorded in $\frac{1}{2}$-h segments, and the O 1s core level was measured often.

Sharp anion core levels were used to align the spectra in Fig. 1 to facilitate comparison of anion-derived valence-band structure. The spectrum of metallic YS (which contains no 4f electrons) shown in Fig. 1(a) yields the relative cross section and relative positions of the S 3s band at 13 eV, the valence band (VB) at 4 eV formed mainly from the S $3p^4$ and Y $5s^2$ electrons, and the Y 4d conduction band. The spectrum of the semiconductor SmS in Fig. 1(b) differs from that of YS in three ways: (1) no 4d conduction band is observed, (2) strong emission from the localized Sm 4f electrons falls in the energy gap between the VB and the conduction band, and (3) two small peaks occur at about 8 and 10 eV. The 4f multiplet structure is characteristic of the final 4f hole states which yield distinctively different spectra for the Sm^{+2} (f^6) and Sm^{+3} (f^5d) initial-state configurations. The expected separations and relative intensities[7] for the multiplet structure from Sm^{+2} are drawn in Fig. 1(b) and are seen to agree well with the 4f structure observed for SmS. The position of the SmS VB can be approximated by comparison with the YS spectrum.

The VB spectrum of SmAs in Fig. 1(c) is composed of the As 4s band at 11 eV, the 4f multiplet characteristic of a Sm^{+3} initial state in the range 4 to 11 eV, and the VB between 0 and 5 eV. The expected separations and intensities[7] [Fig. 1(c)] of the 4f multiplet structure are once again in good agreement with those observed. Comparison of the Sm^{+3} 4f multiplet structure seen for SmAs with the SmS spectrum suggests that the small features at about 8 and 10 eV *might* be associated with a small amount of Sm^{+3} in SmS. In this case a Sm^{+3} line at 6 eV is identical with the shoulder on the side of the valence p-band emission with a peak at 4.2 eV. This assignment would yield a $U(^5I \rightarrow {}^6H)$ of 5.3 eV. However this association is not definitive and all that can definitely be said is that there is $\lesssim 15\%$ Sm^{+3} in Sms.

The results for the ternary system $SmAs_{0.18}S_{0.82}$ at 295 K (solid curve) and 110 K (dotted curve) are shown in Fig. 1(d). It is immediately evident by comparing this spectrum with those in Figs. 1(b) and 1(c) that 4f multiplet hole-state structure characteristic of both Sm^{+3} and Sm^{+2} initial states is present. Also one observes that at 110 K the area ratio of Sm^{+3} to Sm^{+2} multiplets decreases relative to that in the 295-K spectrum. This ratio obtained after subtracting arsenic-derived [not shown in Fig. 1(d)] and sulfur-derived orbital structure and an inelastic background was used to determine the intermediate valence. The Sm^{+3} multiplet area was multiplied by $\frac{6}{5}$ to account for there being one less 4f electron in the Sm^{+3} initial state than in the Sm^{+2} initial state. The assumption that the photoelectric cross section per 4f electron is equal for both $4f^5$ and $4f^6$ configurations should be quite good since both states are localized. The interconfiguration mixing ratios R obtained in this way are listed in Table I.

The spectra of the cation-substituted ternary system $Sm_{0.81}Y_{0.19}S$ in Fig. 1(e) exhibits a similar mixed valence and mixed-valence change with temperature. Spectroscopic estimates of the interconfiguration mixing ratio and intermediate valence at 295 and 110 K are summarized in Table I.

It should be noted that $U(^5I \rightarrow {}^6H)$ of $SmAs_{0.18}S_{0.82}$

TABLE I. Lattice constants a_0 used to calculate effective intermediate valences v_a, and XPS-determined interconfiguration mixing ratios $R = \frac{6}{5} f^5/f^6$ used to calculate effective intermediate valences $v_{XPS} = 2 + R/(1+R)$.

	Lattice constant $a_0 \pm 0.002$ (Å)		$v_a \pm 0.05$		XPS $v_{XPS} \pm 0.05$		R	
	295 K	110 K	295 K	110 K	295 K	110 K	295 K	110 K
SmS	5.966	5.954	2.08		<2.15		<0.18	
$Sm^{+2}S$ [a]	6.00 [a]	5.99 [b]	2.00 [c]	2.00 [c]				
$Sm^{+3}S$ [a]	5.62 [a]	5.61 [b]	3.00 [c]	3.00 [c]				
SmAs	5.914	5.905			3.00	3.00	∞	∞
YS	5.495	5.49 [b]						
$SmAs_{0.18}S_{0.82}$	5.736	5.794	2.83	2.66	2.80	2.68	4.05	2.15
$Sm_{0.81}Y_{0.19}S$	5.687	5.783	2.70	2.36	2.58	2.38	1.38	0.61

[a] Derived. See text. [b] Estimated contraction. [c] Defined.

and $Sm_{0.81}Y_{0.19}S$ is 6.2 eV which is 0.9 eV larger than that deduced for SmS by using the above tentative assignment of $4f^5$ final-state multiplet structure. This observation, coupled with the closing of the gap between the Fermi level and the $4f^6$ structure in SmS on going to $Sm_{0.81}Y_{0.19}S$, is consistent with the $4f^6$ level being destabilized in the intermediate-valence phase by a mechanism such as that described in the Falicov-Kimball model.[8]

Lattice constants as a function of temperature are plotted for SmS, SmAs, $SmAs_{0.18}S_{0.82}$, and $Sm_{0.81}Y_{0.19}S$ in Fig. 2. SmS and SmAs upon cooling exhibit normal contraction while $SmAs_{0.18}S_{0.82}$ and $Sm_{0.81}Y_{0.19}S$ (the same crystals as used in the XPS measurements) expand upon cooling—the latter crystal expanding discontinuously at 160 K. The lattice constant is a sensitive measure of valence (configuration) since the ionic radius of $Sm(4f^6)^{+2}$ is 18% greater than that of $Sm(4f^5)^{+3}$.

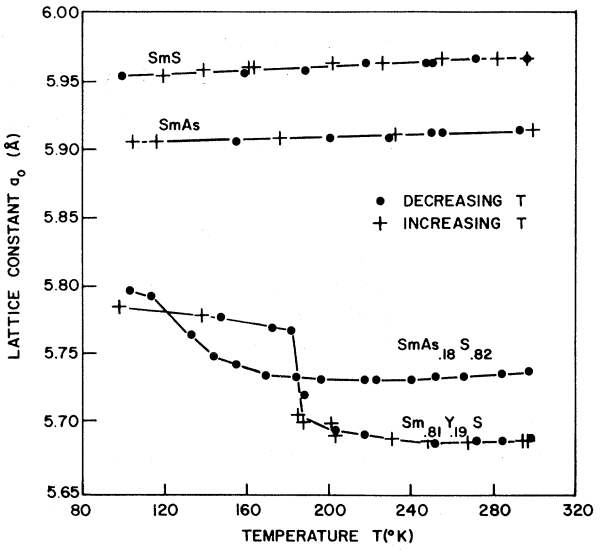

FIG. 2. Lattice constant versus temperature of SmS, SmAs, $SmAs_{0.18}S_{0.82}$, and $Sm_{0.81}Y_{0.19}S$.

Assuming linear hard-sphere mixing one obtains the effective valence

$$v(x) = \left(\frac{a_2^{\mathrm{SmS}} - x[a_2^{\mathrm{SmS}} - a(x=1)] - a(x)}{a_2^{\mathrm{SmS}} - x[a_2^{\mathrm{SmS}} - a(x=1)] - a_3^{\mathrm{SmS}} - x[a_3^{\mathrm{SmS}} - a(x=1)]} \right)(1-P) + (2+P)$$

for cation-substituted ($Sm_{1-x}C_xS$) and anion-substituted (SmA_xS_{1-x}) samarium sulfide, where $a(x)$ is the lattice constant of the solid solution with concentration x. P is zero for cation-substituted solutions and $P=x$ for anion-substituted solutions. The lattice constants a_3^{SmS} for pure trivalent SmS and a_2^{SmS} for pure divalent SmS are derived from a linear extrapolation of lattice constants of neighboring rare-earth sulfides.[9] The compositions of the solid solutions were measured with ± 3% accuracy by electron microprobe spectroscopy. The lattice constants and resulting calculated valences are listed in Table I.

In summary we have quantitatively compared the temperature- and composition-dependent effective valence of $SmAs_{0.18}S_{0.82}$[10] and $Sm_{0.19}Y_{0.81}S$ measured by XPS with values derived from a combination of lattice-constant measurements, electron microprobe analyses, derived lattice constants for divalent and trivalent SmS, and the assumption of hard-sphere mixing. The agreement of v_{XPS} obtained from the electronic density of states and v_a obtained from lattice constants is *direct* evidence that configuration mixing is responsible for the anomalous temperature- and composition-dependence of the lattice constant.

The authors thank J. Kuptsis for the electron microprobe analysis of the SmS solid solutions and P. G. Lockwood for technical assistance.

*Work supported in part by the U.S. Air Force Office of Scientific Research under Contract No. F4462070-C0089.

[1]A. Jayaraman, V. Narayanamurti, E. Bucher, and R. G. Maines, Phys. Rev. Lett. 25, 368 (1970).

[2]M. B. Maple and D. Wohlleben, Phys. Rev. Lett. 27, 511 (1971).

[3]A. Jayaraman, E. Bucher, P. D. Dernier, and L. D. Longinotti, Phys. Rev. Lett. 31, 700 (1973).

[4]F. Holtzberg, in *Magnetism and Magnetic Materials —1973*, AIP Conference Proceedings No. 18, edited by C. D. Graham, Jr., and J. J. Rhyne (American Institute of Physics, New York, 1974), p. 478.

[5]L. L. Hirst, Phys. Kondens. Materie 11, 255 (1970).

[6]M. Campagna, E. Bucher, G. K. Wertheim, D. N. E. Buchanan, and L. D. Longinotti, Phys. Rev. Lett. 32, 885 (1974).

[7]J. L. Freeouf, D. E. Eastman, W. D. Grobman, F. Holtzberg, and J. B. Torrance, Phys. Rev. Lett. 33, 161 (1974).

[8]E. Bucher, V. Narayanamurti, and A. Jayaraman, J. Appl. Phys. 42, 1741 (1971); B. Alascio and A. Lopez, Solid State Commun. 14, 321 (1974), and references therein.

[9]A. Iandelli, in *Rare Earth Research*, edited by E. V. Kleber (MacMillan, New York, 1961).

[10]Lattice-constant measurements of collapsed $SmAs_xS_{1-x}$ samples with increasing x ($x \gtrsim 0.1$) suggest that the intermediate valence increases until it reaches 3 at about $x=0.7$. This system with intriguing *variable* intermediate valence is now being explored.